Transactions of the Korean Nuclear Society Autumn Meeting
Gyeongju, Korea, October 29-30, 2015

Preliminary Thermohydraulic Analysis of a New Moderated Reactor Utilizing an LEU-Fuel for Space Nuclear Thermal Propulsion

Seung Hyun Nam[a*], Jae Young Choi[a], Paolo F. Venneri[a], Yong Hoon Jeong[a], Soon Heung Chang[a,b]
[a]*Department of Nuclear and Quantum Engineering, Korea Advanced Institute of Science & Technology, 291 Daehak-ro, Yuseong-gu, Daejeon 34141, Republic of Korea*
[b]*Handong Global University, 558 Handong-ro, Buk-gu, Pohang, Gyeongbuk 37554, Republic of Korea*
[*]*Corresponding author: rashkid@kaist.ac.kr*

1. Introduction

A Nuclear Thermal Rocket (NTR) is a viable and promising option for human deep-space exploration due to its high thrust and efficiency, proven technology, bimodal capability, and safe and reliable performance for the time being. The state-of-the-art NTR designs mostly use a fast or epithermal neutron spectrum core, loading a Highly-Enriched Uranium (HEU) fuel to make a high power reactor with a minimum-size and simple core. However, the HEU-NTRs inevitably provoke nuclear proliferation obstacles on all R&D activities by civilians and non-nuclear weapon states, and eventual commercialization [1]. To overcome these obstacles, a new NTR design utilizing a Low-Enriched Uranium (LEU) fuel is required, but it minimizes performance degradation due to the heavy LEU fuel loading.

The Korea Advanced NUclear Thermal Engine Rocket utilizing an LEU fuel (KANUTER-LEU) is a non-proliferative and comparably efficient NTR engine with relatively low thrust levels of 40 ~ 50 kN for in-space transportation. The small modular engine can expand mission versatility, when flexibly used in a clustered engine arrangement, so that it can perform various scale missions from low-thrust robotic science missions to high-thrust manned missions. In addition, the clustered engine system can enhance engine redundancy and ensuing crew safety as well as the thrust. As depicted in Fig. 1, the engine system mainly consists of an Extremely High Temperature Gas cooled Reactor utilizing an LEU fuel (EHTGR-LEU), a propulsion system using H_2 propellant and an optional Electricity Generation System (EGS).

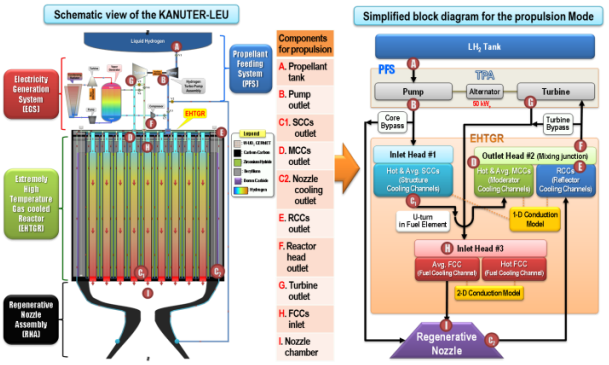

Fig. 1. Schematic view and simplified block diagram of the KANUTER-LEU.

The propulsion system is an energy conversion system to transform the thermal energy of the reactor into the kinetic energy of the propellant to produce the powers for thrust, propellant feeding and electricity. It is mainly made up of a propellant Feeding System (PFS) comprising a Turbo-Pump Assembly (TPA), a Regenerative Nozzle Assembly (RNA), etc. For this core design study, an expander cycle is assumed to be the propulsion system. In the expander cycle, the H_2 propellant flows through the various components of the system both for cooling the EHTGR and the RNA, and for transferring the heat to the energy conversion systems of the TPA and the thermodynamic nozzle. The liquid H_2 in propellant tanks is drawn through a pump of the TPA. The pump sends the pressurized H_2 flow to cooling channels in secondary reactor components (moderator, reflector, RNA, etc.) to extract the heat for the propellant feeding power. After cooling the secondary reactor components, the accessorily heated H_2 flows up to the TPA to drive its turbine. The H_2 then flows into primary fuel assemblies in the core and is exhausted through the thermodynamic nozzle to generate rocket thrust. Table 1 presents the design parameters of the KANUTER-LEU. The NTR engine could be optionally modified to be a bimodal engine for both propulsion and electricity generation by equipping the EGS schematically shown in Fig. 1. The EGS converts the thermal energy of the EHTGR in the idle operation (only 350 kW_{th} power) to electric power during the electric power mode.

This paper presents a preliminary thermohydraulic design analysis to explore the design space for the new reactor and to estimate the referential engine performance.

2. Moderated EHTGR Utilizing LEU Fuel

The EHGTR-LEU is an energy source for operating the propulsion system and the EGS, which heats the H_2 propellant by fission energy without core melting. To efficiently implement a heavy LEU fuel for the NTR engine, the reactor design innovatively possesses the key characteristics of the high U density fuel with the resistances against high heating and H_2 corrosion, the thermal neutron spectrum core, and the compact reactor design with protectively cooling capability. Table 2 presents the design parameters and criteria of the EHTGR-LEU.

Table Ⅰ. Design parameters of the KANUTER-LEU.

Categories	Parameters
Engine mass budgets (excluding the EGS)	
EHTGR[a,b] (200 ~ 250 MW_{th})	712 ~ 722 kg
Shadow shield & auxiliaries[b]	249 ~ 253 kg
Propulsion system	260 kg
- Turbo-pump assembly	41.5 kg
- Propellant management	63.7 kg
- Thrust vector control	11.9 kg
- Instrumentation	10.0 kg
- Regenerative nozzle assembly	132.8 kg
Total engine[b]	1,221 ~ 1,235 kg
Rocket performance (at a nozzle expansion ratio of 200)	
Chamber temperature[d] (mixed mean)	2,640 ~ 2,760 K
Chamber pressure	6.895 MPa
Pump discharge pressure[b,d]	< 16 MPa
System pressure drop[b,d]	< 9 MPa
Thrust[c]	40 ~ 52 kN
T/W_{eng} ratio[c]	3.1 ~ 4.3
I_{sp}[d]	860 ~ 904 s
Optional electricity generation (350 kW_{th})	
Power cycle	Brayton or Rankine
Net power output[e]	25 ~ 55 kW_e
Radiator size[e]	7.9 ~ 3.2 m^2/kW_e

[a]The reactor mass is estimated with $ZrH_{1.8}$ moderator.
[b]Depending on a pitch to diameter ratio of fuel element.
[c]Mainly depending on a reactor power.
[d]Mainly depending on a fuel assembly geometry (channel size).
[e]Depending on a type of power conversion cycle.

Table Ⅱ. Design parameters and criteria of the EHTGR-LEU.

Categories	Parameters
Reactor power (at electric power mode)	200 ~ 250 MW_{th} (350 kW_{th})
Avg. fuel power density[a,b]	10.2 ~ 14.0 MW_{th}/liter
Number of fuel elements	61
Pitch to diameter ratio of fuel element	1.66 ~ 1.76
Fuel type	^{184}W-UO_2 CERMET
- U enrichment	19.5 wt% $^{235}U/U$
- Fuel mass (^{235}U mass)[b]	282 ~ 251 kg (18.7 ~ 16.6 kg)
- Fuel assembly geometry	Square lattice with various channel sizes
Moderator type and mass[b]	$ZrH_{1.8}$ & 134 ~ 156 kg
Reflector (PV) type and mass (including 12 control drums)	Be – Be – C/C, B_4C & 254 kg
Structural comp. and mass	Be, C/C & 52 kg
Total reactor mass[b]	722 ~ 712 kg
Reactor diameter and height (core diameter and height)	66 & 61 cm (50.4 & 50.4 cm)
Peak fuel centerline temperature[c]	≤ 2,920 K
Peak moderator temperature[a,b]	≤ 850 K
Avg. fuel exit H_2 temperature[c]	2,500 ~ 2,770 K
Core pressure drop[b,c]	< 2.8 MPa
Operation time at the max. power	2 hours

[a]Depending on a reactor power.
[b]Depending on a pitch to diameter ratio of fuel element.
[c]Depending on a fuel assembly geometry (channel size).

2.1 Integrated Fuel Element Design

The nuclear fuel selection is one of the key issues to utilize LEU in the fuel. The fuel should be able to keep not only high U density, but also great resistance to ultra-high thermal and H_2 corrosion attacks in the core. There are two types of fuels that have potential to meet the requirements, which are carbide based fuels and CERMET (CERamic-METallic) fuels [2]. In the view point of U content in fuels, the CERMET fuels have 3 ~ 5 times higher U density (≤ 6.5 g/cm^3) than that of the carbide fuels (≤ 2.5 g/cm^3) and so could be a feasible fuel option for the EHTGR-LEU. Particularly, the Uranium Dioxide imbedded in Tungsten matrix (W-UO_2) CERMET fuel is one of the greatly promising options for the EHTGR [2]. The CERMET fuel consists of a 45 vol% W with the remainder being UO_2 with a 6 mol% ThO_2 bonding agent and thus has a great U density of about 5 g/cm^3. The ^{235}U enrichment of the fuel is assumed to be 19.5 w/o as an LEU typically used in research reactors and so rates a fissile material density of 0.97 g/cm^3. The CERMET fuel can also increase safety margin due to comparably high melting points, great thermal conductivity, better creep strength, excellent hot H_2 corrosion endurance and good fission product retention [2,3]. To mitigate the neutron absorption by the W matrix, the W is needed to be enriched to 95 a/o ^{184}W whose thermal absorption cross-section is significantly lower than that of other W isotopes [4].

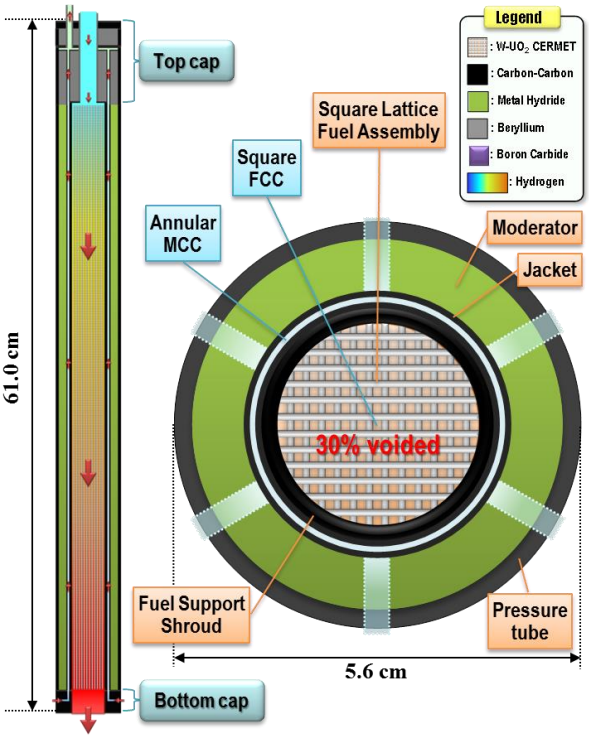

Fig. 2. Configuration of the integrated fuel element.

The ^{184}W-UO_2 CERMET fuel is manufactured in the wafer forms having the thicknesses from 0.50 mm to 1.50 mm. The fuel wafers are interlocked with each other and supported by the heat-resistant shroud to build the peculiar fuel assembly with the square lattice geometry as shown in Fig. 2. The square lattice fuel design is originally proposed by the Innovative Nuclear Space power & Propulsion Institute (INSPI) to enhance

the heat transfer capability and to reduce the fabrication difficulties [5]. The square lattice fuel geometry creates numerous square Fuel Cooling Channels (FCCs), maintaining 30% cross-sectional void fraction of the fuel assembly to ensure sufficient coolant passages and a critical fuel mass. This square lattice design is very simple and cost-effective in terms of fabricability, compared to typical hexagonal fuel design with circular cooling channels. In addition, the numerous micro-size FCCs are able to improve heat transfer between the fuel and coolant due to increasing the heat transfer area and resultantly decreasing the heat flux of the fuel.

The integrated fuel element uniquely houses the fuel assembly, moderator block, protectively cooling channels and structural components such as fuel support shroud and individual pressure tube as an all-in-one package as observed in Fig. 2 The square lattice fuel assembly is supported and surrounded by the three layers of moderator and pressure tubes according to the structural and thermal design considerations in order of first, the carbon fiber-reinforced carbon composite (C/C) shroud protectively coated with zirconium carbide (ZrC) to support the high temperature fuel assembly, second, the metal hydride moderator block protected by the thin ZrC-coated C/C jacket, and third, the individual C/C pressure tube. The main moderator is absolutely crucial to enable the LEU fuel use in the EHTGR because it is able to largely reduce heavy metal demand to be a critical reactor. A serious challenge to use the hydride moderators in the very high temperature core is to sufficiently cool them for prevention of melting and large H_2 dissociation. So, the fuel element also contains the annular Moderator Cooling Channel (MCC) between the first and second layers to protect the hydride moderator from the thermal attacks of the fuel and radiation induced heating. The integrated design involves both functions of NERVA-derived fuel and tie-tube elements such as sufficient heat transfer for energy conversion and structural support. In addition, it is also able to efficiently increase room for moderator in the core and to mitigate stress load to the reactor's Pressure Vessel (PV) by the individual pressure tube [6]. The relative amounts of fuel and moderator are regulated by Pitch to Diameter ratio (P/D) of the fuel element.

2.2 Moderated and Compact Reactor Design

The suitable moderator candidates are the metal hydrides such as lithium-7 hydride (^{7}LiH) or zirconium hydride ($ZrH_{1.8}$). ^{7}LiH not only has a high neutron scattering cross-section in the thermal energy range due to its high hydrogen content (12.68 wt% H), but also a comparable melting temperature, a low dissociation pressure (~ 2.66 kPa at its melting point) and a low density [7,8]. However, its poor thermal properties such as low thermal conductivity and high thermal expansion coefficient are critical issue to have to be resolved for a feasible reactor design. Additionally, to use LiH as a moderator, very high isotopic enrichment of ^{7}Li is required because even a small inclusion of ^{6}Li causes a large reactivity penalty [4]. Another very promising candidate is $ZrH_{1.8}$, having a higher melting temperature, thermal conductivity and mechanical strength [9,10], although its neutron moderating performance relative to density is worse than that of ^{7}LiH. Hense, ^{7}LiH is more efficient moderator in terms of neutronics and weight, whereas $ZrH_{1.8}$ has much better robustness regarding thermo-mechanical properties to overcome the particular conditions of the very high temperature and pressure core. In addition, ZrH was actually used and demonstrated as a moderator for some space reactors such as Topaz-2 and SNAP series for decades [11]. In these regards, $ZrH_{1.8}$ is the baseline moderator for the EHTGR-LEU in this study.

The 61 integrated fuel elements, housing the moderator, are arranged in the hexagonal prism pattern core with the Beryllium (Be) spacers as shown in Fig. 3. The Be spacers have the Structure Cooling Channels (SCC) to cool the structural components and the moderator at the outside of the fuel elements. The compact core is surrounded by the reflector composed of the Be – Be – C/C layers to reduce neutron leakage. Particularly, the outer Be – C/C reflector also serves as the reactor's PV [6]. To control the reactor's reactivity and in turn the power, rotating cylindrical control drums, each of which partially comprises a Boron Carbide (B_4C) neutron absorber, are symmetrically placed in the radial reflector. The reflector and control drums also have the various Reflector Cooling Channels (RCCs) for cooling and regeneration.

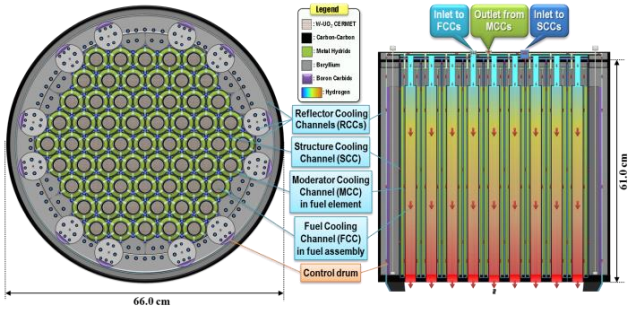

Fig. 3. Configuration of the EHTGR-LEU.

Overall, the EHTGR-LEU has such integrated and compact design, which efficiently houses the fuel, moderator, reflector, control and structural components to increase the amount of moderator and to maintain the structural integrity in a minimum size. In addition, it evenly distributes the protectively and regeneratively cooling channels in the core such as the FCCs for fuel, MCCs and SCCs for moderator, and RCCs for reflector. The various cooling channels mitigate severe heating of the reactor components, whereas increase the coolant enthalpy to regeneratively transfer the thermal energy to the energy conversion systems for both propulsion and electricity generation. The size and mass of the EHTGR-LEU are estimated to be an outer diameter of 66 cm and a mass between 712 kg and 722 kg according to a P/D of the fuel element at constant sizes of the fuel element, core

and reflector. The comparable reactor mass despite using LEU, compared with other NERVA derived HEU-reactors, is mainly due to reduction of fuel loading in the thermal neutron energy spectrum core, and employment of the lightweight and high-strength structural materials. The maximum power of reactor is 250 MW_{th} in the propulsion mode and the idle power is 350 kW_{th} in the electric power mode.

The previous neutronic analysis indicates that this reactor design has sufficient design space in terms of criticality and burn up in the P/D range of 1.66 ~ 1.76. At a referential P/D of 1.68, the EHTGR-LEU has the K_{eff} range of 1.011 ~ 0.960 with the reactivity swing of $ 7.1 according to the control drum directions, the fuel power density of 12.7 MW_{th}/liter at the 250 MW_{th} power and the reactor mass of 720 kg. Table 3 summarizes the component-level heat deposition of the EHTGR-LEU with 250 MW_{th} power. Fig. 4 shows the fuel power distribution according to position in the core.

Table Ⅲ. Reactor heat deposition at 250 MW_{th} power.

Components	Energy deposition [MW_{th}]	Fraction
Fuel	239.38	0.957
Moderator	5.44	0.022
Core supporting structures	1.89	0.008
Reflector and CDs[a]	3.29	0.013
Total	250.00	1.000

[a]CDs, control drums.

3. Preliminary Thermohydraulic Design Analysis

The thermohydraulic analysis was carried out to explore design space of the proposed reactor design and to resultantly estimate rocket performance of the KANTUER-LEU engine in consideration of the design criteria: maximum fuel centerline temperature, maximum moderator temperature and core pressure drop. Both to be a feasible design and to create high rocket performance, the heat generated in the reactor must be sufficiently removed and simultaneously the power density and fuel exit coolant temperature should be as high as possible within the design criteria. In this respect, this study focuses on cooling performance of the various protectively cooling channels for fuel and moderator in the core. The component-level heat deposition data of the EHTGR-LEU, summarized in Table 3, is applied to this analysis. Additionally, to describe the power distribution in the core, the power profiles, normalized to the average, is also considered with the heat deposition data. The study consists of the fuel element P/D effect analysis, the reactor power effect analysis and the fuel assembly geometry effect analysis in accordance with the primary design parameters. For the design criteria, the maximum centerline temperature of fuel was determined to be the constant 2,920 K, which considers about 200 K margin to the local melting temperature of UO_2 as a conservative upper limit on reactor temperature. The maximum temperature of $ZrH_{1.8}$ moderator was set to be under 850 K to prevent melting (about 220 K margin) and large H_2 dissociation. The H_2 dissociation pressure of $ZrH_{1.8}$ at 850 K is predicted to be just about 9.2 kPa. The limit of the core pressure drop should be set depending on the structural considerations of the fuel element, but currently there is no structural analysis result on that. So, only for a referential purpose, the limit of the maximum core pressure drop was set to be 2.8 MPa, applying the maximum value of the CERMET NTR reactor designs in the GE-710 program [12,13].

3.1 Methodology

The thermohydraulic analysis was performed by using both an in-house NTR engine system code as a main means and the 3-D Computational Fluid Dynamics (CFD) code, ANSYS CFX [14], as an auxiliary means for result validation of the new thermofluid dynamic model on the major core components. The new computational NTR engine model, Nuclear Square-channel-core in Expander-cycle Simulation (NSES), simulates and analyzes an expander cycle engine system with the complex EHTGR [15]. The NSES currently focuses on thermohydraulic analysis of the unique reactor core design during the propulsion mode in steady-state to estimate feasible design points and resultant rocket performance. Hense, the analysis model can particularly describe the reactor design features of the peculiar square lattice fuel geometry and the integrated fuel element configuration with the various protectively and regeneratively cooing channels.

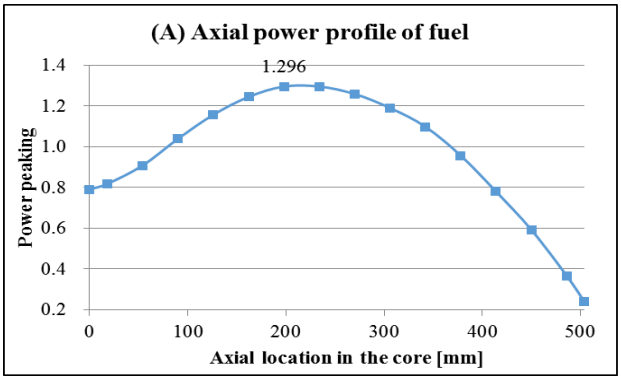

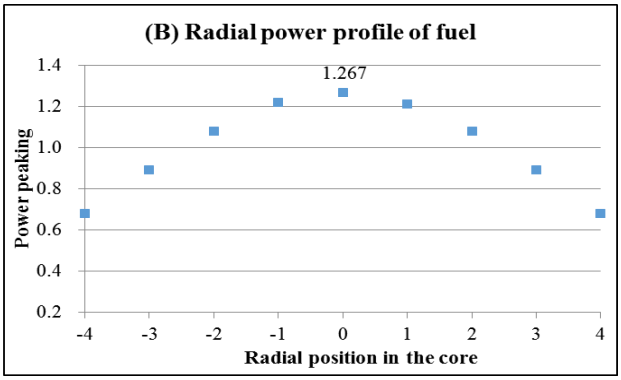

Fig. 4. Fuel power distribution according to position in the core.

The propulsion system is simply modeled as an expander cycle with the major components of the PFS and RNA, as shown in Fig. 1, to obtain the input information for the reactor analysis and to estimate the theoretical engine performance, including pump discharge pressure (system pressure), pressure drop, chamber state, thrust, T/W_{eng}, I_{sp}, etc. The NSES includes a 1-D thermodynamic model to estimate propellant state and rocket performance of the entire engine system, and heat transfer models for the reactor components with heat generation. The heat transfer models consist of 2-D and 1-D radial thermal conduction models, incorporated with empirical local convective heat transfer correlations. The 2-D heat transfer model is used to precisely estimate temperature distribution of the fuel and the 1-D heat transfer model is applied to roughly predicting temperature distribution of the other reactor components, including the moderator, reflector, etc. The code is written in MATLAB [16].

Fig. 5. Computational analysis process of the NSES.

Fig. 5 briefly presents the computational analysis process of the NSES. The code iteratively solves the thermofluid dynamic models for the expander cycle engine system with the complex EHTGR, based on user-defined initial conditions. The input data includes maximum fuel temperature in the hot-channel, average chamber pressure, reactor power, required electric power, both coolant bypass ratios before the inlets of the core and the turbine, P/D of the fuel element, size of the unit FCC in the square lattice fuel assembly, base dimensions of the system components, etc. For this parametric analysis, the constant values of the input data are set to be the maximum fuel temperature of 2,920 K, the chamber pressure of 6.895 MPa, the required electric power of 50 kW_e, the same bypass ratios of 0.10 and the base dimensions of the engine system. In particular, both maximum fuel temperature and chamber pressure act as the governing constraints for convergence of the iterative calculation. Then, the main parameters are the P/Ds of 1.66 ~ 1.80, the reactor powers of 200 ~ 250 MW_{th} and the unit FCC sizes, consistently related with the five Fuel Wafer Thicknesses (FWT) of 0.50 ~ 1.50 mm. The iterative calculation ends when both governing constraints meet their target values. The final outputs are system Mass Flow Rate (MFR), propellant thermodynamic state of the entire system, thermal state of the reactor components and resultant rocket performance such as thrust, T/W_{eng} and I_{sp}.

A few representatively selected results on the major core component analysis, involving the integrated fuel element with the FCC, MCC and SCC, were compared with the results of the 3-D CFD (CFX) analysis. The CFD analysis can more precisely simulate the thermo-fluid dynamics of the core component flow with the complex geometry. All the input conditions for the CFD analysis, including the geometry, heat deposition, MFR and boundary conditions, are consistent with those of the NSES analysis.

3.2 Result

3.2.1 Fuel element P/D effect analysis result

For the P/D effect analysis, the reactor power and the FWT (unit FCC size) are applied to be the constant values of 250 MW_{th} and 0.75 mm. The P/D of the fuel element determines not only the volume ratio between the fuel and moderator, but also the cross-sectional flow areas of the FCCs and the MCC in the integrated fuel element with the constant diameter and height. The increase in P/D makes low the cross-sectional flow areas of the FCCs and the MCC in the fuel elements, and correspondingly brings down the Heat Transfer Areas (HTA) of both cooling channels in the core as shown in Fig. 6. The HTA decrease of the FCC augments the heat flux on the channel wall and resultantly increases the system MFR to maintain the constant maximum fuel temperature.

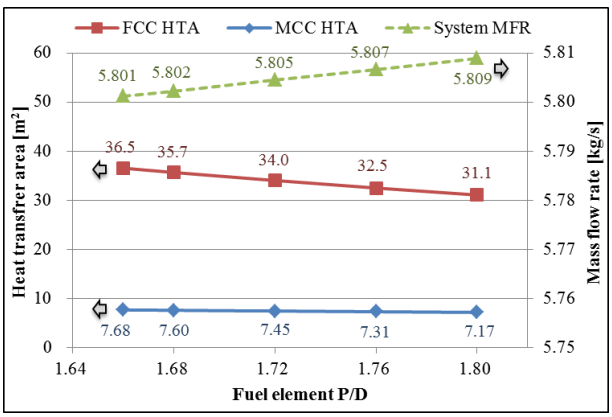

Fig. 6. HTAs of the MCCs and FCCs in the core versus system MFR as a function of P/D at 250 MW_{th} power and 0.75 mm FWT.

In case of the MCC, the lower HTA causes the higher moderator temperature in spite of the slightly increased MFR. Fig. 7 shows the temperatures in the central (hottest) fuel element and the chamber as a function of P/D. The maximum value of the peak moderator temperatures is calculated to be only 591 K at a P/D of 1.80. Actually, the calculated value by the simplified 1-D conduction model is about 10 % underestimated, compared with the result of the 3-D CFD analysis, due to neglecting gradients in radial heat concentration. So, the corrected value is predicted to be about 650 K, which still has a sufficient margin of 420 K to prevent melting the $ZrH_{1.8}$ moderator. At the peak moderator temperature, the H_2 dissociation pressure of just 9E-03 kPa is also negligible.

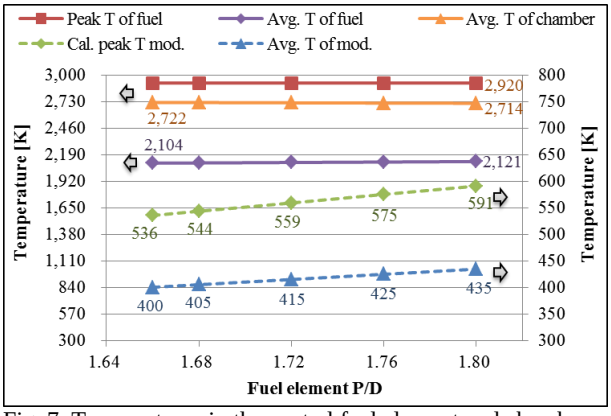

Fig. 7. Temperatures in the central fuel element and chamber as a function of P/D at 250 MW_{th} power and 0.75 mm FWT.

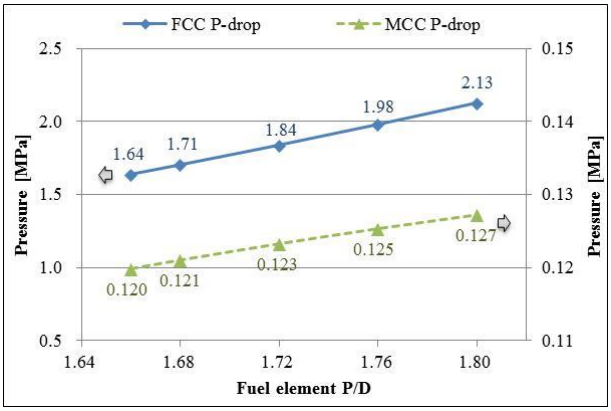

Fig. 8. Pressure drops in the central fuel element as a function of P/D at 250 MW_{th} power and 0.75 mm FWT.

The mixed mean chamber temperature slightly decreases according to the P/D rise because of the increase in MFR. In case of pressure drop in the central fuel element, depicted in Fig. 8, the higher P/D increases both pressure drops of FCC and MCC due to the reduction of the cross-sectional flow areas and the increase in MFR. The maximum value of the core pressure drops is also estimated to be 2.13 MPa at a P/D of 1.80 and corresponding pump discharge pressure is rated to be 14.4 MPa. The thrust and T/W_{eng} slightly increase in accordance with the rise in P/D because of both increase in MFR and loss in reactor weight, whereas the I_{sp} shows a little reduction due to the decrease in chamber temperature as observed in Fig. 9. Consequentially, the P/D primarily affects the moderator temperature and core pressure drop, and even their maximum values are under the design criteria in the P/D range of 1.66 ~ 1.80.

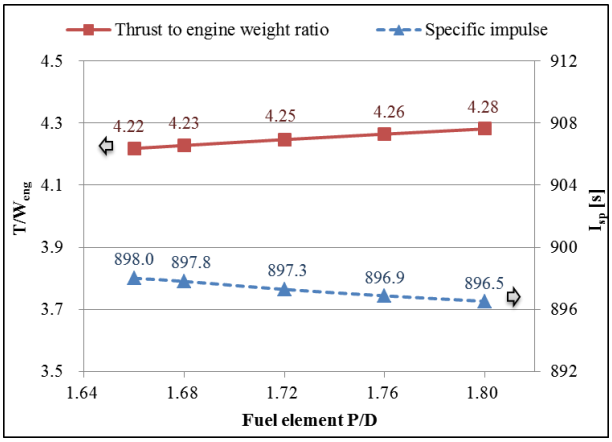

Fig. 9. T/W_{eng} and I_{sp} as a function of P/D at 250 MW_{th} power and 0.75 mm FWT.

3.2.2 Reactor power effect analysis result

The reactor power effect analysis was performed in the power range of 200 ~ 250 MW_{th}, and the constant P/D and FWT of 1.68 and 0.75 mm, respectively. The increase in power means higher power density of the components and correspondingly elevated heat flux on the walls of cooling channels. In particular, the high power density in the fuel increases MFR to maintain the constraint of perk fuel temperature, and again the increase in MFR augments pressure drop and corresponding pump discharge pressure as shown in Fig. 10. The maximum core pressure drop and pump discharge pressure are rated to be 1.71 MPa and 13.49 MPa at the highest power of 250 MW_{th}, and the pressure drop is lower than the hypothetical limit.

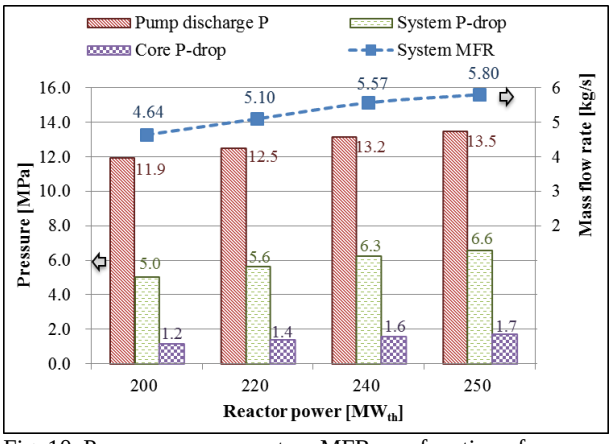

Fig. 10. Pressures versus system MFR as a function of power at 1.68 P/D and 0.75 mm FWT.

Fig. 11 presents the temperatures in the central fuel element and the chamber as a function of reactor power. The average temperatures in fuel and moderator slightly

increase due to the rise in power density, whereas the chamber temperatures are estimated to be a similar value of around 2,725 K because of the corresponding MFR rising. Hense, the thrust and T/W_{eng} are augmented according to the rises in the power and ensuing MFR as observed in Fig. 12, whereas the I_{sp} ,which mainly depend on the chamber temperatures, are similar in the range of 898 ~ 901 s. These indicate that the powers up to 250 MW_{th} could be included in potentially feasible design space, creating the thrust range of 41 ~ 51 kN.

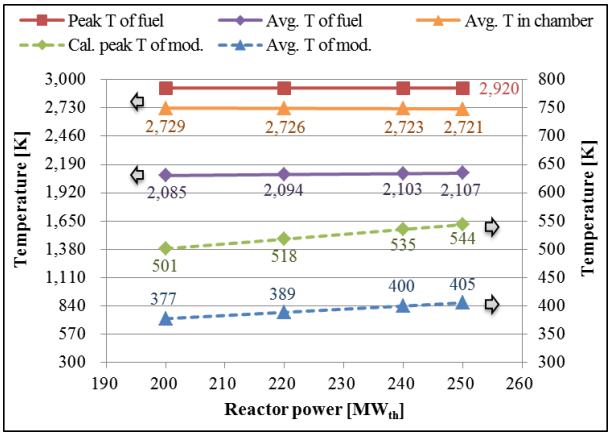

Fig. 11. Temperatures in the central fuel element and chamber as a function of power at 1.68 P/D and 0.75 mm FWT.

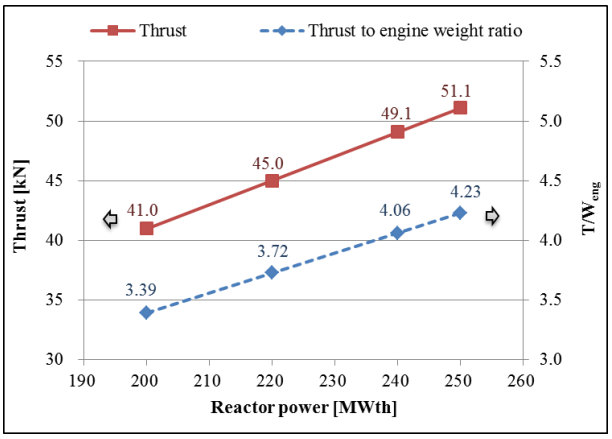

Fig. 12. Thrust and T/W_{eng} as a function of power at 1.68 P/D and 0.75 mm FWT.

3.2.3 Fuel assembly geometry effect analysis result

The fuel geometry effect analysis was carried out on the various sizes of FCC with the FWTs from 0.50 mm to 1.50 mm to investigate the cooling performance of the square lattice fuel assembly design. For the analysis, the P/D and the reactor power are applied to be the constant values of 1.68 and 250 MW_{th} to estimate the maximum rocket performance. As the characteristic of the square lattice design, the FWTs are respectively related with the values of 0.607 ~ 1.794 mm in width for the square FCC and the corresponding number of FCCs to maintain the constant cross-sectional flow area fraction of 30 % in the fuel assembly. Fig. 13 shows the number of FCCs and their Heat Transfer Area (HTA) in the core as a function of FWT.

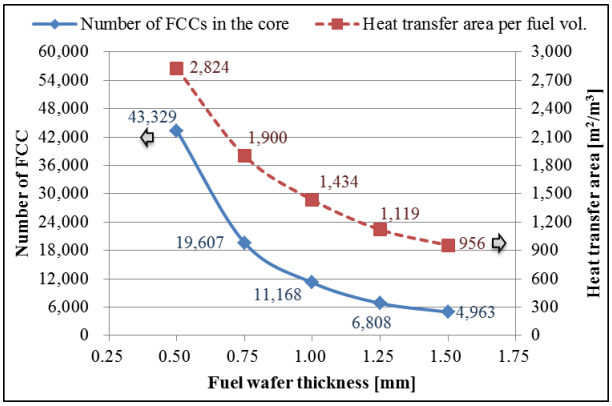

Fig. 13. Number of FCCs and HTA in the core as a function of FWT.

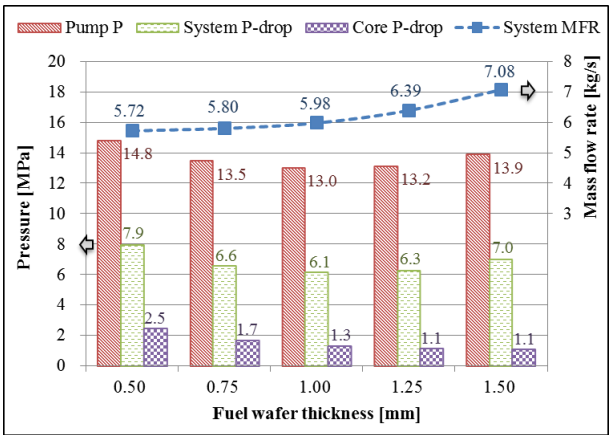

Fig. 14. Pressures versus system MFR as a function of FWT at 250 MW_{th} power and 1.68 P/D

As can be seen, the higher FWT, correspondingly creating larger channel size, exponentially decreases the number of FCCs and ensuing HTA in the constant fuel volume. This indicates that the increase in FWT largely augments heat flux on the FCC walls even in constant power density of fuel. Again, the rise in heat flux elevates the system MFR to keep the peak fuel temperature as depicted in Fig. 14. Although the MFR increases according to the fuel thickening, the core pressure drop lessens instead due to the overwhelming decline in the HTA. The maximum values of the core pressure drops and the pump discharge pressures are estimated to be 2.49 MPa and 14.84 MPa, respectively, at the thinnest FWT of 0.50 mm. The minimum pressure drop of core is estimated to be 1.08 MPa at the thickest FWT of 1.50 mm and the minimum system pressure is rated to be only 13.0 MPa at a FWT of 1.00 mm. Fig. 15 presents the temperatures in the central fuel element and the chamber as a function of FWT. The increases in both heat flux and ensuing MFR according to the fuel thickening cause that the chamber temperature decreases, whereas the average fuel temperature increases. In case of the moderator temperature, both peak and average values slightly diminish due to the MFR rising in accordance with the fuel thickening.

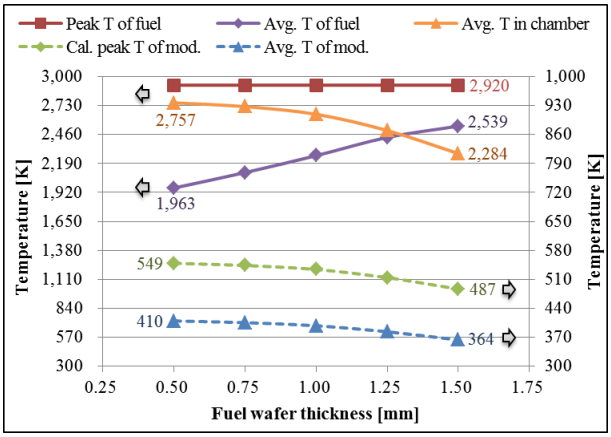

Fig. 15. Temperatures in the central fuel element and chamber as a function of FWT at 250 MW_{th} power and 1.68 P/D.

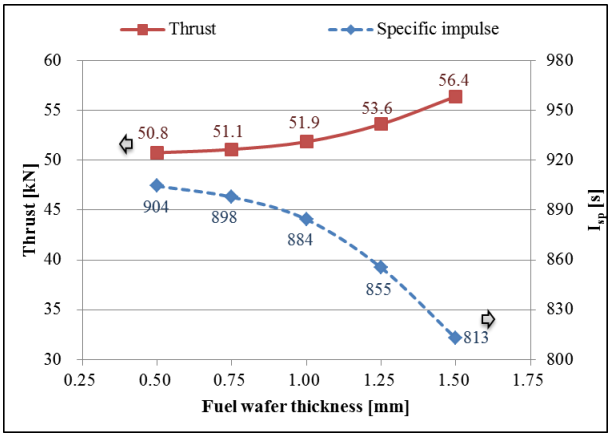

Fig. 16. Thrust and I_{sp} as a function of FWT at 250 MW_{th} power and 1.68 P/D.

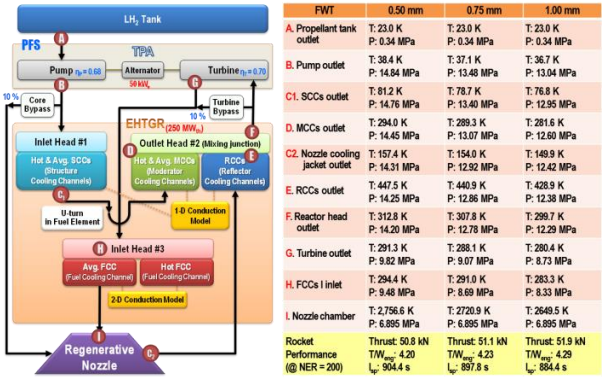

FWT	0.50 mm	0.75 mm	1.00 mm
A. Propellant tank outlet	T: 23.0 K P: 0.34 MPa	T: 23.0 K P: 0.34 MPa	T: 23.0 K P: 0.34 MPa
B. Pump outlet	T: 38.4 K P: 14.84 MPa	T: 37.1 K P: 13.48 MPa	T: 36.7 K P: 13.04 MPa
C1. SCCs outlet	T: 81.2 K P: 14.76 MPa	T: 78.7 K P: 13.40 MPa	T: 76.8 K P: 12.95 MPa
D. MCCs outlet	T: 294.0 K P: 14.45 MPa	T: 289.3 K P: 13.07 MPa	T: 281.6 K P: 12.60 MPa
C2. Nozzle cooling jacket outlet	T: 157.4 K P: 14.31 MPa	T: 154.0 K P: 12.92 MPa	T: 149.9 K P: 12.42 MPa
E. RCCs outlet	T: 447.5 K P: 14.25 MPa	T: 440.9 K P: 12.86 MPa	T: 428.9 K P: 12.38 MPa
F. Reactor head outlet	T: 312.8 K P: 14.20 MPa	T: 307.8 K P: 12.78 MPa	T: 299.7 K P: 12.29 MPa
G. Turbine outlet	T: 291.3 K P: 9.82 MPa	T: 288.1 K P: 9.07 MPa	T: 280.4 K P: 8.73 MPa
H. FCCs I inlet	T: 294.4 K P: 9.48 MPa	T: 291.0 K P: 8.69 MPa	T: 283.3 K P: 8.33 MPa
I. Nozzle chamber	T: 2,756.6 K P: 6.895 MPa	T: 2720.9 K P: 6.895 MPa	T: 2649.5 K P: 6.895 MPa
Rocket Performance (@ NER = 200)	Thrust: 50.8 kN T/W_{eng}: 4.20 I_{sp}: 904.4 s	Thrust: 51.1 kN T/W_{eng}: 4.23 I_{sp}: 897.8 s	Thrust: 51.9 kN T/W_{eng}: 4.29 I_{sp}: 884.4 s

Fig. 17. Propellant thermodynamic states in the engine system according to FWTs of 0.50 ~ 1.00 mm.

The maximum value of the calculated peak moderator temperatures is just 549 K, which is about 10 % underestimated, at the thinnest FWT. Hense, as the FWT get thicker, the thrust and corresponding T/W_{eng} are augmented, whereas the I_{sp} drops due to the MFR rising and the corresponding chamber temperature falling as shown in Fig. 16. The highest thrust and T/W_{eng} are rated to be 56.5 kN and 4.57 at the thickest FWT. On the contrary, the maximum I_{sp} is estimated to be 904 s at the thinnest FWT. These indicates that a fuel assembly with a thinner fuel is thermally robust and more efficient against less structural strength, while a fuel assembly with a thicker fuel is structurally strong with lower pressure drop, reducing the axial shear stress. So, an optimum FWT should balance both thermal and structural considerations to maximize rocker performance [5]. To satisfy the design criteria, presented in Tables 1 and 2, the potential design space for the fuel geometry involves the FWT range of 0.50 ~ 1.25 mm, creating around 52 kN thrust, 4.3 T/W_{eng} and 860 ~ 900 s I_{sp}. Fig. 17 presents the propellant thermodynamic state of the engine system according to the FWTs of 0.50 ~ 1.00 mm.

3.3 Discussion

In summary, to keep the governing constraints of the constant peak fuel temperature and chamber pressure, the fuel element P/D mainly affects moderator temperature and core pressure drop, and the reactor power has major effects on system MFR and corresponding pressure drop and thrust. In case of the fuel assembly geometry effect analysis, the size of the FCCs in the unique square lattice fuel assembly largely affects the amount of heat flux on the FCC walls, system MFR, core pressure drop, fuel exit temperature and corresponding overall rocker performance, including propellant efficiency (I_{sp}). The result indicates that the potentially feasible design space, satisfying the major design parameters and criteria, involves the P/D range of 1.66 ~ 1.76, the power range of 200 ~ 250 MW_{th} and the FWT range of 0.50 ~ 1.25 mm. A referential design point in the design space is selected to be a P/D of 1.68, a reactor power of 250 MW_{th} and a FWT of 0.75 to representatively show a result validation and a referential mission performance. The selection of the design point primarily considers both sufficient reactor control margin and high rocker performance, excluding the maximum values in this analysis.

The result validation for the NSES analysis was performed by comparison with the result of the CFD (CFX) analysis, and focused on the major core components, involving the integrated fuel element with the FCC, MCC and SCC. Figs. 18 and 19 show the temperature profiles of the propellant, fuel and moderator along the cooling channels at the referential design point to compare both results from the NSES and the CFX. In case of the fuel component analysis, the errors of local propellant state along the FCC are in ranges of 0.08 ~ 0.36 % for bulk temperature and -0.13 ~ 0.04 % for pressure. The local centerline temperature of fuel has an error range of 0.06 ~ 11.30 % and a Mean Absolute Error (MAE) of 4.10 % as observed in Fig. 18. The peak fuel temperature of the CFX result is estimated to be 2,915 K, which is 0.17 % lower than that of the NSES result (2,920 K). As can be seen in Fig. 19, the moderator component analysis shows that the errors of local propellant state along the MCC are in the ranges of -1.12 ~ 3.11 % for bulk temperature and -0.02 ~ 0.04 % for pressure. The local average temperature of

moderator has an error range of -0.79 ~ 3.68 %, but in case of the local maximum temperature, the errors are relatively large in a range of -1.77 ~ -10.40 % (7.29 % MAE). The peak moderator temperature of the CFX result is rated to be 594 K, which is about 9.2 % higher than that of the NSES result (544 K). These large errors in local maximum temperature of moderator are because the CFX more precisely analyzes the temperature gradients by radial heat concentration than the NSES. Therefore, the peak moderator temperatures, underestimated by the NSES, should be conservatively weighted, compared to the result of the CFD analysis.

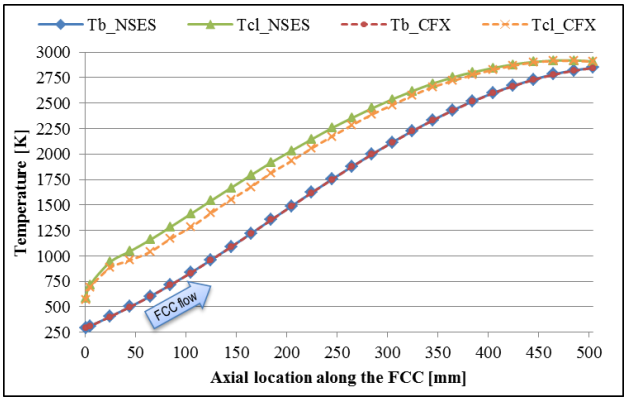

Fig. 18. Temperature profiles of propellant and fuel along the FCC from both NSES and CFX.

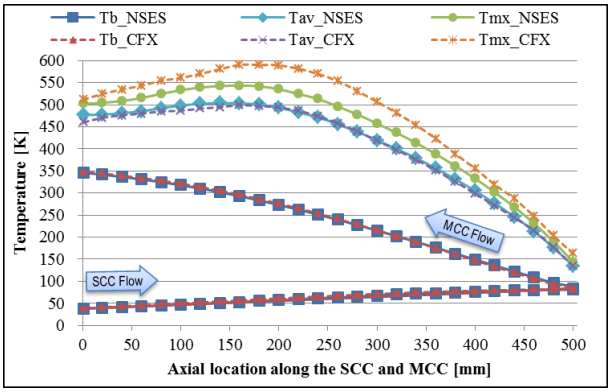

Fig. 19. Temperature profiles of propellant and moderator along the SCC and MCC from both NSES and CFX.

4. Conclusion

The new non-proliferative NTR engine concept, KANUTER-LEU, is under designing to surmount the nuclear proliferation obstacles on all R&D activities and eventual commercialization for future generations. To efficiently implement a heavy LEU fuel for the NTR engine, its reactor design innovatively possesses the key characteristics of the high U density fuel with high heating and H_2 corrosion resistances, the thermal neutron spectrum core and also minimizing non-fission neutron loss, and the compact reactor design with protectively cooling capability. In consideration of the key concepts, the EHTGR-LEU primarily adapts the ^{184}W-UO_2 CERMET fuel, $ZrH_{1.8}$ moderator, C/C and Be structural components, and its core is mainly composed of the integrated fuel elements and various protectively cooling channels for high performance and compactness in this study. The EHTGR-LEU also could be bimodally operated for both of propulsion and electricity generation.

To investigate feasible design space for the moderated EHTGR-LEU and resultant engine performance, the preliminary design analyses of neutronics and thermo-hydraulics were carried out with the assumption of an expander cycle in steady-state. The result demonstrates that the feasible design space for the reactor design potentially involves the P/D range of 1.66 ~ 1.76, the power range of 200 ~ 250 MW_{th} and the FWT range of 0.50 ~ 1.25 mm to meet the major design parameters and criteria. Accordingly, the referential rocket performance are estimated to be in the range of 11.94 ~ 14.84 MPa in maximum system pressure, the thrust range of 41.0 ~ 53.6 kN, the T/W_{eng} range of 3.39 ~ 4.44 and the I_{sp} range of 855.4 ~ 904.4 according to the major parameters. The performance of the KANUTER-LEU is comparable with that of the existing HEU-NTR engines in spite of the heavy LEU fuel loading according to the mission performance comparison.

In future, more extensive and integrated design analyses, including neutronics, thermohydraulics, structural analysis and their coupling analysis will be conducted for validation and optimization of the new reactor design. In addition, a transient analysis is also essential to validate the reactor operations during startup and power changes for the bimodal capability.

REFERENCES

[1] P. Venneri, Implementation of LEU Fuels in NERVA type Nuclear Thermal Rockets, KAIST, 2013.

[2] S.K. Bhattacharyya, An Assessment of Fuels for Nuclear Thermal Propulsion, Argonne, IL, USA, 2001.

[3] D. Burkes, D. Wachs, J. Werner, S. Howe, An Overview of Current and Past W-UO2 CERMET Fuel Fabrication Technology, in: Proceedings of Space Nuclear Conference 2007, INL, Boston, MA, USA, 2007: pp. 207–216.

[4] G. Rosaire, P. Husemeyer, P. Venneri, W. Deason, Design of a Low_Enriched Nuclear Theraml Rocket, ID, USA, 2013.

[5] S. Anghaie, T.W. Knight, J. Plancher, R. Gouw, Development of a Robust Tri-Carbide Fueled Reactor for Multi-Megawatt Space Power and Propulsion Applications, Innovative Nuclear Space Power and Propulsion Institute (INSPI), University of Florida, Gainesville, FL, USA, 2004.

[6] J. Powell, J. Paniagua, G. Maise, H. Ludewig, M. Todosow, The Role of Compact Nuclear Rockets in Expanding the Capability for Solar System Science and Exploration, State University of New York at Stony Brook/TR-740, Stony Brook, NY, USA, 1997.

[7] R. E. Hyland, Reactor-Weight Study of Beryllium Oxide, Beryllium, Lithium-7 Hydride, and Water as Moderators with

Tungsten184 Structural Material and Uranium Dioxide Fuel, NASA-TN-D-1407, 1962.

[8] F.H. Welch, Lithium hydride: A space age shielding material, Nuclear Engineering and Design. 26 (1974) 444–460. doi:10.1016/0029-5493(74)90082-X.

[9] S. Yamanaka, K. Yamada, K. Kurosaki, M. Uno, K. Takeda, H. Anada, et al., Characteristics of zirconium hydride and deuteride, Journal of Alloys and Compounds. 330-332 (2002) 99–104. doi:10.1016/S0925-8388(01)01448-7.

[10] M.P. Puls, Properties of Bulk Zirconium Hydrides, in: Springer London, London, 2012. doi:10.1007/978-1-4471-4195-2.

[11] A.K. Hyder, R.L. Wiley, G. Halpert, D.J. Flood, S. Sabripour, Spacecraft Power Technologies, Imperial College Press, Covent Garden, London, 2000. doi:10.1142/9781860947773.

[12] J. Walton, An overview of tested and analyzed NTP concepts, 1991.

[13] C.W. Bills, 710 High-Temperature Gas Reactor Program Summary Report. Volume I. Summary, Cincinnati, OH, US, 1967. doi:10.2172/4338293.

[14] ANSYS Inc., ANSYS CFX Tutorials, 15317 (2010).

[15] S.H. Nam, J. young Choi, P.F. Venneri, Y.H. Jeong, S.H. Chang, Thermohydraulic Design Analysis Modeling for Korea Advanced NUclear Thermal Engine Rocket for Space Application, in: Transactions of the Korean Nuclear Society Spring Meeting, KNS, Jeju, Korea, 2015.

[16] MathWorks, MATLAB, (2014).